On the Importance of Viscoelastic Response Consideration in Structural Design Optimization

Kai A. James[a], Haim Waisman[b]

[a] *University of Illinois at Urbana-Champaign, Department of Aerospace Engineering, Urbana, Illinois, United States; tel: 217-300-3270; fax: 217-244-0720; kaijames@illinois.edu*

[b] *Columbia University, Department of Civil Engineering and Engineering Mechanics, New York, New York, United States*

Abstract

In this paper we present a series of mathematical proofs that demonstrate the importance of accounting for viscoelastic effects in structural optimization algorithms. Focusing specifically on mass minimization problems with stiffness and deflection constraints, we show that standard techniques based on linear elastic analysis overestimate the long-term stiffness of the structure, leading to designs that become infeasible after sustained loading due to viscoelastic creep. Conversely, assuming maximum creep deflection, which also allows for linear analysis, leads to an overly conservative design that is unnecessarily heavy and therefore suboptimal. We prove both propositions for both constant and time-varying load histories. We also present proofs for generalized continuum mechanics problems as well as for a finite element formulation, which can be applied to any arbitrary geometry. Lastly, we present two numerical examples in which the conclusions derived in the proofs are verified empirically.

Keywords: structural optimization; viscoelasticity; creep deformation; finite element analysis

1. Introduction

Viscoelasticity is the property by which solid materials exhibit time-dependent responses when subject to sustained loading. While many engineering materials are known to have significant and observable viscoelastic behavior, particularly when operating at high temperatures, most structural

design optimization procedures fail to take this property into account, and instead treat the structural material properties as being independent of time. Because of the time-dependent nature of viscoelastic materials, they are often used in structural damping applications, and there have been a number of studies on viscoelastic design optimization of structures subject to dynamic loading [1, 2, 3, 4, 5, 6]. However, few have tackled the problem of structural design while accounting for unwanted viscoelastic effects such as creep deformation. In this paper, we explore the design of structures subject to sustained loading that is either constant, or varies on a time scale that is slow enough that all inertial effects are negligible. When subject to these types of loads, viscoelastic structures exhibit creep deformation in which the deflection of the structure increases gradually, with the rate of increase slowing down over time.

A recent study by the authors [7] explored the use of viscoelastic analysis in topology optimization algorithms for designing structures, while taking into account undesirable creep effects, in order to improve long-term structural performance. Through several numerical examples, it was shown that structures that were designed under the assumption of linear elasticity, became infeasible and failed to meet the design requirements when the structure's long-term performance was evaluated using a linear viscoelastic model. Similarly, the examples showed that when the authors attempted to account for viscoelastic effects by implementing a simplified *worst-case* viscoelastic model, the resulting structure was over-designed and was therefore suboptimal. The solution was to incorporate time-dependent viscoelastic analysis into the structural optimization algorithm, in order to achieve a structure that was both feasible and optimal for the specific load duration or operating time for which the structure was to be designed. The current paper extends upon the previous study by presenting formal mathematical proofs of the observations and conclusions of that study. These proofs further highlight the importance of accounting for viscoelastic effects in the design of static structures comprised of viscoelastic material.

2. The Linear Viscoelastic Model

In the current paper, as well as in the previous study [7], the material is assumed to exhibit linear viscoelasticity. From the principle of Boltzmann superposition, one can deduce the following viscoelastic stress-strain relation for a time-varying axially applied stress, evaluated at time t .

$$\sigma(t) = \int_0^t E(t-s)\frac{\partial \varepsilon(s)}{\partial s}\mathrm{d}s. \tag{1}$$

where E is the relaxation modulus or relaxation function, and s is a dummy variable representing the domain over which the integral is evaluated . This function is an intrinsic property of the material and is typically determined by fitting experimental data [8]. When used to describe one-dimensional axial loading, the parameter E is referred to as the extensional relaxation function. This quantity is analogous to the elasticity modulus used to describe stiffness in elastic materials. Alternatively, one can describe the viscoelastic behavior of a material using the creep compliance function, D, which is the inverse of the relaxation function. When a viscoelastic material is subject to constant loading the strain history of the material response follows the path of the creep compliance function. The two functions are related to one another via the following equation.

$$\int_0^t D(t-s)\frac{\partial E(s)}{\partial s}\mathrm{d}s = 1 \tag{2}$$

Figure 1 contains examples of typical relaxation and creep functions. Note that each function begins at an initial value which reflects the instantaneous (purely elastic) response of the material. The functions then increase or decrease monotonically as they asymptotically approach the final or *worst-case* value (as $t \to \infty$). Note that in this context, the "worst case" refers to a loading scenario in which the load is held constant, at its maximum magnitude for infinite time, which leads to maximum creep deflection. This load case is useful since it provides conservative approximation of the the structural deflection (as we will demonstrate in the following sections), and the response can be easily computed using a linear elastic analysis In the case of the relaxation function, the decrease represents a gradual loss of stiffness as the material"relaxes" over time. Conversely, the increasing trajectory of the creep compliance function reflects the gradual increase in strain or deflection of the viscoelastic material over time.

For multidimensional viscoelastic analysis, we require time-dependent functions for both the shear and bulk moduli, K and G respectively. For practical reasons it is often the case that only extensional relaxation data

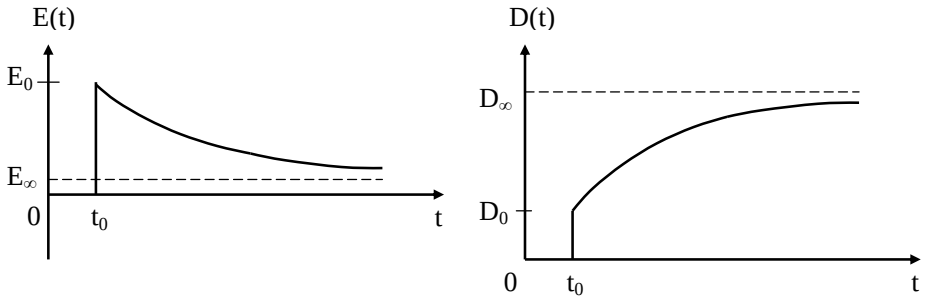

(a) Relaxation function (c) Creep function

Figure 1: Examples of typical relaxation and creep functions

are available, and therefore one must extrapolate this data to obtain shear and bulk modulus functions [9]. Depending on the material, the viscoelastic behavior in shear and in bulk may differ significantly, however a common approach is to assume synchronicity in between the two functions [10, 11]], so that

$$K(t) = \beta G(t). \tag{3}$$

where β is a constant scalar multiplier. Under this assumption, the full viscoelastic response of the material can be captured by a single relaxation modulus [12]. Therefore it is convenient to employ to a constitutive law based on the Young's modulus and the Poisson ratio, since ν reduces to a constant $\nu = \nu_0$, and the extensional relaxation modulus, $E(t)$ can be treated as being mathematically equivalent to the time-dependent Young's modulus, E_{Y}. For a general two- or three-dimensional problem, the linear viscoelastic stress-strain relation is given by

$$\boldsymbol{\sigma}(t) = \int_0^t \mathbf{C}(t-s)\frac{\partial \boldsymbol{\varepsilon}(s)}{\partial s}\mathrm{d}s. \tag{4}$$

where $\boldsymbol{\sigma}$ and $\boldsymbol{\varepsilon}$ are the stress and strain tensors respectively, and $\mathbf{C}(t)$ is the time-dependent elasticity tensor given by $\frac{E(t)}{E_0}\mathbf{C}_0$, where $\mathbf{C}_0$, is the initial (maximum stiffness) elasticity prior to the onset of relaxation . Note

that this relation applies specifically to linear elastic materials that obey the Boltzmann superposition principle. For simplicity the proofs that follow are based this synchronous viscoelastic model.

3. Viscoelastic Modeling and Structural Optimization

The previous paper [7] investigated structural optimization problems in which the objective was to minimize the structural mass, subject to a constraint on the maximum deflection due to creep measured at some target time t^*. The optimization problem can be written mathematically as follows

$$\begin{aligned} &\min_{\mathbf{x}} \ \sum_{e=1}^{N_e} a_e x_e \\ &\text{subject to: } u(t^*) \leq u^*, \end{aligned} \tag{5}$$

where x_e are generic structural design variables that could represent material densities in the case of topology optimization problems, or cross-sectional areas in the case of discrete truss structures. The coefficients a_e represent specific geometric properties of the structural elements. In the case of topology optimization, a_e represents the element volume, and in the case of discrete truss elements, a_e represents the element length, so that, when multiplied by the design variables, the resulting product is proportional to the mass of the element. The variable u represents the local displacement at a given location, and this value is constrained so that it does not exceed the target displacement u^*.

In the previous study, it was observed that, when solving the above design problem, assuming linear elasticity leads to an insufficiently stiff structure, whose deflection overshoots its target value once viscoelasticity is taken into account. Similarly, design based on a worst-case scenario assumption causes the optimizer to over-design the structure, making it unnecessarily heavy. Here we offer a mathematical proof that this observation will hold in general for any minimum-mass optimization procedure involving isotropic linear viscoelastic material. These two extreme cases (elastic and worst-case) are significant benchmarks, since both can be evaluated rapidly using linear elastic analysis. However, through the proofs presented below, we demonstrate that both techniques are flawed since they yield structural designs that are either infeasible, or suboptimal.

In order to state the problem mathematically, we express the viscoelastic displacement, u, as a function of the design variable vector $\mathbf{x}$, and the time, t. Note that u is a scalar quantity corresponding to the displacement at the specific location (or degree of freedom) at which we seek to enforce the constraint during the optimization. Furthermore, let $\mathbf{x}_{\text{elastic}}$ represent the structure that is optimized so that its deflection meets the target deflection value, u^*, when analyzed under the assumption of elasticity. Therefore

$$u(\mathbf{x}_{\text{elastic}}, t_0) = u^* \tag{6}$$

where t_0 is the initial time at which the load is first applied. Similarly, let $\mathbf{x}_{\text{worst}}$ represent the structure that is optimized so that its deflection meets the target deflection value, u^*, under the worst-case assumption (i.e. $t \to \infty$ and $\mathbf{F}(t) = \mathbf{F}_{\text{max}}$ for all t, where $\mathbf{F}_{\text{max}}$ is the maximum value reached by the actual time-dependent force history function). Therefore

$$u(\mathbf{x}_{\text{worst}}, \infty)|_{\text{F=F}_{\text{max}}} = u^* \tag{7}$$

Lastly, let $\mathbf{x}_{\text{visc}}$ represent the structure that is optimized using viscoelastic analysis so that

$$u(\mathbf{x}_{\text{visc}}, t^*) = u^*, \quad \text{for} \quad t_0 < t^* < t_\infty \tag{8}$$

Where $t^* \in (t_0, \infty)$ is the critical time for which the structure is to be designed. Using these definitions, we shall prove the following inequalities.

$$|u(\mathbf{x}_{\text{worst}}, t^*)| < |u^*| < |u(\mathbf{x}_{\text{elastic}}, t^*)|, \quad \text{for} \quad t^* > t_0 \tag{9}$$

Note that in the above inequality, the elastic design and worst case design are evaluated based on their respective deflections at time t^*, using a time-dependent viscoelastic analysis in which $t^* - t_0$ is some finite, non-zero time duration. Note also that in the limiting case where $t^* = t_0$ the viscoelastic analysis is equivalent to an elastic analysis so that $u(\mathbf{x}_{\text{elastic}}, t^*) = u^*$. In the remaining subsections we prove this relation for both constant and time-varying loads.

4. Constant Loading

In the case of constant loading, the proof is trivial. One need simply observe that

$$u(\mathbf{x}, t) = u(\mathbf{x}, t_0)\frac{D(t)}{D_0}, \quad \text{with} \quad \frac{D(t)}{D_0} > 1 \quad \text{for all} \quad t > 0. \tag{10}$$

Note that this statement makes no assumptions about the geometry or discretization of the problem. From here, one can easily deduce that $|u(\mathbf{x}_{\text{elastic}}, t^*)| > |u^*|$, for $t^* > t_0$. Therefore, the full proof, along with the proof of the first half of the general proposition pertaining to the worst-case design are left as exercises for the reader.

5. Time-Varying Loads

5.1. One-Dimensional Problems

In this section we derive analogous proofs for a general, time-varying proportional load. We initially derive the proofs for a simple one-dimensional axial load problem, and in Section 5.2 we show how these proofs can be extended to apply to any arbitrary geometry using a finite element formulation. In the case of a one-dimensional geometry with axial loading, the load can be expressed using the scalar σ, which represents the applied stress. Similarly, the strain state can be captured using the scalar ε. Note that we restrict the proofs to loads in which the force does not change direction (i.e. $\sigma(t) > 0$ for all $t > t_0$), which is a reasonable assumption for many support structures. For all loads satisfying this description, we wish to prove that the actual viscoelastic displacement for a structure optimized based on a linear elastic model is greater than the target displacement for which the structure was designed. Similarly, we shall prove that for a structure optimized using a worst-case analysis, the actual viscoelastic displacement is smaller than the target displacement, u^*, for which the structure was designed, thus making the design suboptimal. For increased simplicity, we make use of the fact that the axial displacement is directly proportional to the axial strain (i.e. $u = \varepsilon L$, where L is the axial length of the undeformed structure. Therefore the general proposition can be written in terms of the axial strains as follows.

$$\varepsilon(\mathbf{x}_{\text{worst}}, t^*) < \varepsilon^* < \varepsilon(\mathbf{x}_{\text{elastic}}, t^*) \tag{11}$$

By proving the above inequality, we implicitly prove the proposition expressed in 9. All proofs assume linear viscoelasticity and therefore the Boltzmann superposition equation applies.

From the known characteristic of the the relaxation function, we can derive two properties that will assist in the proof. First we note that since E is a monotonically decreasing function (see Fig. 1a), we can assert the following.

$$\textbf{lemma } ① : \text{ if } t_1 < t_2, \text{ then } E(t_1) > E(t_2) \tag{12}$$

Secondly, from the Boltzmann equation 1, one can deduce the following

$$\textbf{lemma } ② : \text{ if } \sigma(t) \geq 0 \text{ for all } t, \text{ then } \varepsilon(t) \geq 0 \text{ for all } t \tag{13}$$

Although this latter observation appears to be intuitive, its proof is non-trivial. Therefore, below we present a proof, which uses integration by parts. We begin with the complementary form of the Boltzmann superposition equation in which the time-dependent strain function $\varepsilon(t)$ is expressed as a function of the stress history and the creep compliance function $D(t)$ as follows.

$$\varepsilon(t) = \int_0^t D(t-s)\frac{\partial \sigma(s)}{\partial s}\mathrm{d}s \tag{14}$$

Integrating by parts, we obtain

$$\varepsilon(t) = \left[D(t-s)\sigma(s)\right]_0^t - \int_0^t \left[\frac{\partial}{\partial s}D(t-s)\right]\sigma(s)\mathrm{d}s \tag{15}$$

The first term in the above expression must be greater that zero since both $D(t)$ and $\sigma(t)$ are positive for all times t. Turning to the integral term, we note that

$$\frac{\partial}{\partial s}D(t-s) = \frac{\partial D(r)}{\partial r}\frac{\partial r}{\partial s}, \text{ where } r = t-s; \tag{16}$$

From Figure 1b, we see that $\frac{\partial D(r)}{\partial r} > 0$ for all r, and since $\frac{\partial r}{\partial s} = -1$, we can deduce that $\frac{\partial}{\partial s} D(t - s) < 0$ for all s and t. Also, since $\sigma(s)$ is strictly positive for all s, we have shown that the second term in Eqn. 15 is also positive. Therefore $\varepsilon(t) > 0$ for all t, and the proof of Lemma 2 is complete.

From here, we proceed to the latter portion of the general proposition (11), which pertains to designs optimized using linear elasticity. We must show that

$$\varepsilon^* < \varepsilon(\mathbf{x}_{\text{elastic}}, t^*). \tag{17}$$

According to linear elasticity, the stress-strain relation is given by

$$\sigma(t^*) = E_0 \varepsilon_{\text{elastic}}(\mathbf{x}_{\text{elastic}}, t^*), \tag{18}$$

For any structure designed to satisfy the deflection constraint given in Eqn. 5, under the assumption of linear elasticity, the elastic strain will be equal to the target strain, i.e. $\varepsilon_{\text{elastic}}(\mathbf{x}_{\text{elastic}}, t^*) = \varepsilon^*$. Therefore, we can deduce a relationship between the target strain, ε^*, and the actual viscoelastic strain, ε, of the structure represented by $\mathbf{x}_{\text{elastic}}$ as follows.

$$\begin{aligned} E_0 \varepsilon^* = \sigma(t^*) &= \int_0^{t^*} \theta(s) \frac{\partial \varepsilon(s)}{\partial s} \mathrm{d}s \\ \Rightarrow \varepsilon^* &= \int_0^{t^*} \frac{\theta(s)}{E_0} \frac{\partial \varepsilon(s)}{\partial s} \mathrm{d}s \qquad (19) \\ &= \int_0^{t^*} \frac{\partial \varepsilon(s)}{\partial s} \mathrm{d}s - \int_0^{t^*} \left(1 - \frac{\theta(s)}{E_0}\right) \frac{\partial \varepsilon(s)}{\partial s} \mathrm{d}s \\ &= \varepsilon(t^*) - \int_0^{t^*} \left(1 - \frac{\theta(s)}{E_0}\right) \frac{\partial \varepsilon(s)}{\partial s} \mathrm{d}s \qquad (20) \end{aligned}$$

Note that in the above equations, we have omitted the $\mathbf{x}$ variable for improved clarity, however it is implied above, as well as for the remainder of the proof, that $\varepsilon(t^*) = \varepsilon(\mathbf{x}_{\text{elastic}}, t^*)$. Rearranging to isolate the viscoelastic strain term, $\varepsilon(t^*)$, and integrating by parts we obtain

$$\varepsilon(t^*) = \varepsilon^* + \left[\left(1 - \frac{\theta(s)}{E_0}\right)\varepsilon(s)\right]_0^{t^*} - \int_0^{t^*}\left(-\frac{\partial\theta(s)}{\partial s}\right)\varepsilon(s)\mathrm{d}s$$
$$= \varepsilon^* + \left(1 - \frac{\theta(t^*)}{E_0}\right)\varepsilon(t^*) + \int_0^{t^*}\frac{\partial\theta(s)}{\partial s}\varepsilon(s)\mathrm{d}s \tag{21}$$

Note that, as before, the term $\left(1 - \frac{\theta(0)}{E_0}\right)\varepsilon(0)$ vanishes since $\varepsilon(0) = 0$. Since E_0 represents the peak value of both $E(s)$ and $\theta(s)$, we know that $\frac{\theta(s)}{E_0} \leq 1$, therefore $\left(1 - \frac{\theta(s)}{E_0}\right) \geq 0$. Also, from lemma 2, $\varepsilon(s) > 0$ for all $s > 0$. Lastly $\frac{\partial\theta(s)}{\partial s} > 0$, since $\theta(s)$ is a monotonically increasing function. Therefore, we can write

$$\varepsilon(t^*) = \varepsilon^* + \Pi, \quad \text{where } \Pi > 0, \tag{22}$$

which implies that $\varepsilon(\mathbf{x}_{\text{elastic}}, t^*) > \varepsilon^*$, and thus the proof is complete.

The portion of the proposition pertaining to the worst-case design (i.e. $\varepsilon(\mathbf{x}_{\text{worst}}, t^*) < \varepsilon^*$) is solved in two parts. Here we introduce an intermediate analysis method in which the applied force remains constant at $\tilde{\sigma}(t) = \max(\sigma)$, for all $t > 0$, however we solve for the viscoelastic strain at t^* using a time-dependent analysis. This approach is hereafter referred to as a *partial* worst case analysis, and the strains obtained by this method shall be denoted using $\tilde{\varepsilon}$. Therefore we seek to prove that

$$\varepsilon(\mathbf{x}_{\text{worst}}, t^*) \leq \tilde{\varepsilon}(\mathbf{x}_{\text{worst}}, t^*) < \varepsilon^*. \tag{23}$$

Note that since all strain values apply to the worst case design, $\mathbf{x}_{\text{worst}}$, we again omit the $\mathbf{x}$ variable, so it should be understood that for the remainder of the proof $\varepsilon(t) = \varepsilon(\mathbf{x}_{\text{worst}}, t)$. The first part of the above inequality (i.e. $\varepsilon(t^*) \leq \tilde{\varepsilon}(t^*)$), can proved simply by expressing both strain quantities in the form given in Eqn. 15, which we derived earlier using integration by parts.

$$\varepsilon(t) = \frac{1}{E_0}\sigma(t) + \int_0^t \frac{1}{[\theta(s)]^2}\frac{\partial\theta(s)}{\partial s}\sigma(s)\mathrm{d}s \tag{24}$$
$$\tilde{\varepsilon}(t) = \frac{1}{E_0}\tilde{\sigma}(t) + \int_0^t \frac{1}{[\theta(s)]^2}\frac{\partial\theta(s)}{\partial s}\tilde{\sigma}(s)\mathrm{d}s \tag{25}$$

Noting that $\tilde{\sigma}(t) \geq \sigma(t)$ for all $t > 0$ (from the definition of $\tilde{\sigma}$), one can deduce from inspection that $\tilde{\varepsilon}(t^*) \geq \varepsilon(t^*)$, therefore the proof is complete.

For greater understanding, we present an alternative proof based on mathematical induction. We begin by writing the Boltzmann form of time-dependent applied stress function, σ, and the partial worst-case stress function, $\tilde{\sigma}$, with the integrals expressed as a Riemann sum, in which the differential time increment ds is replaced by a finite time step Δt.

$$\sigma(t^*) = \lim_{\Delta t \to 0} \sum_{i=1}^{n_t} E(t^* - t_i) \Delta \varepsilon_i \tag{26}$$

$$\tilde{\sigma}(t^*) = \lim_{\Delta t \to 0} \sum_{i=1}^{n_t} E(t^* - t_i) \Delta \tilde{\varepsilon}_i, \tag{27}$$

Where $n_t = t^*/\Delta t$ and $\Delta \varepsilon_i > \varepsilon(t_i) - \varepsilon(t_{i-1})$. Since $\tilde{\sigma}(t) \geq \sigma(t)$ for all $t > 0$, we can further assert that

$$\lim_{\Delta t \to 0} \sum_{i=1}^{n_t} E(t^* - t_i) \Delta \varepsilon_i \leq \lim_{\Delta t \to 0} \sum_{i=1}^{n_t} E(t^* - t_i) \Delta \tilde{\varepsilon}_i \tag{28}$$

Let us now assume that the above relation holds true for some consistent discretization of the time domain, which uses a finite time step, $\Delta t > 0$. We can therefore omit the limit term to obtain

$$\sum_{i=1}^{n_t} E(t^* - t_i) \Delta \varepsilon_i \leq \sum_{i=1}^{n_t} E(t^* - t_i) \Delta \tilde{\varepsilon}_i, \tag{29}$$

which holds for all values of n_t. From here we must prove that $\varepsilon(t_{n_t}) \leq \tilde{\varepsilon}(t_{n_t})$, or equivalently

$$\sum_{i=1}^{n_t} \Delta \varepsilon_i \leq \sum_{i=1}^{n_t} \Delta \tilde{\varepsilon}_i, \tag{30}$$

in order to show that $\varepsilon(t^*) \leq \tilde{\varepsilon}(t^*)$. We now proceed with the proof by mathematical induction. For the base case, we prove the above statement with $n_t = 1$. From Eqn. 29 we have

$$E(0)\Delta\varepsilon_1 \leq E(0)\Delta\tilde{\varepsilon}_1. \tag{31}$$

From here, it is trivial to deduce that $\varepsilon(t_1) \leq \tilde{\varepsilon}(t_1)$, therefore the base case is proven. To prove that Eqn. 30 holds for any number of terms n_t we first assume that it holds for $n_t = k$. Therefore

$$\sum_{i=1}^{k} \Delta\varepsilon_i \leq \sum_{i=1}^{k} \Delta\tilde{\varepsilon}_i. \tag{32}$$

Now, based on this assumption, we prove that Eqn. 30 must also hold for $n_t = k + 1$. From Eqn. 29, we have

$$\sum_{i=1}^{k+1} E(t^* - t_i)\Delta\varepsilon_i \leq \sum_{i=1}^{k+1} E(t^* - t_i)\Delta\tilde{\varepsilon}_i. \tag{33}$$

We now decompose both sums as follows.

$$\sum_{i=1}^{k+1} \left[E(0) - (E(0) - E(t_{k+1} - t_i))\right] \Delta\varepsilon_i \leq \sum_{i=1}^{k+1} \left[E(0) - (E(0) - E(t_{k+1} - t_i))\right] \Delta\tilde{\varepsilon}_i \tag{34}$$

Noting that $t_{k+1} - t_i = (k + 1 - i)\Delta t$ the inequality becomes

$$\begin{aligned} E(0)\sum_{i=1}^{k+1} \Delta\varepsilon_i - \sum_{i=1}^{k+1} \left[E(0) - E((k+1-i)\Delta t)\right] \Delta\varepsilon_i \\ \leq E(0)\sum_{i=1}^{k+1} \Delta\tilde{\varepsilon}_i - \sum_{i=1}^{k+1} \left[E(0) - E((k+1-i)\Delta t)\right] \Delta\tilde{\varepsilon}_i \end{aligned} \tag{35}$$

In the latter summation on either side of the inequality, the final term in the summation ($i = k + 1$) vanishes. Therefore, omitting that $k + 1$ term and rearranging the remaining terms in the summation, we arrive at

$$E(0)\sum_{i=1}^{k+1}\Delta\varepsilon_i - \sum_{i=1}^{k}\left[\Big(E((k-i)\Delta t) - E((k+1-i)\Delta t)\Big)\sum_{j=1}^{i}\Delta\varepsilon_j\right]$$
$$\leq E(0)\sum_{i=1}^{k+1}\Delta\tilde{\varepsilon}_i - \sum_{i=1}^{k}\left[\Big(E((k-i)\Delta t) - E((k+1-i)\Delta t)\Big)\sum_{j=1}^{i}\Delta\tilde{\varepsilon}_j\right] \tag{36}$$

Rearranging to isolate the $\varepsilon(t_{k+1})$ and $\tilde{\varepsilon}(t_{k+1})$ terms, we obtain

$$E(0)\left(\sum_{i=1}^{k+1}\Delta\tilde{\varepsilon}_i - \sum_{i=1}^{k+1}\Delta\varepsilon_i\right)$$
$$\geq \sum_{i=1}^{k}\left[\Big(E((k-i)\Delta t) - E((k+1-i)\Delta t)\Big)\sum_{j=1}^{i}\left(\Delta\tilde{\varepsilon}_j - \Delta\varepsilon_j\right)\right] \tag{37}$$

From the assumption, we know that $\Delta\tilde{\varepsilon}_j - \Delta\varepsilon_j > 0$ for all j up to $j = k$. Also, from lemma 1 (Eqn. 12), we know that $E((k-i)\Delta t) - E((k+1-i)\Delta t) > 0$ for all values of i and k. Lastly, we know that $E(0) > 0$, therefore we can conclude that

$$\sum_{i=1}^{k+1}\Delta\tilde{\varepsilon}_i - \sum_{i=1}^{k+1}\Delta\varepsilon_i \geq 0$$
$$\Rightarrow \varepsilon(t_{k+1}) \leq \tilde{\varepsilon}(t_{k+1}) \tag{38}$$

By mathematical induction, this proves that $\varepsilon(t_i) \leq \tilde{\varepsilon}(t_i)$ for all $i > 0$, and therefore the proof is complete.

To prove the second half of the proposition in 23, (i.e. $\tilde{\varepsilon}(\mathbf{x}_{\text{worst}}, t^*) < \varepsilon^*$), we begin with the definition of the worst-case design, $\mathbf{x}_{\text{worst}}$, which is defined as $\mathbf{x}$ such that the viscoelastic strain satisfies $\varepsilon(\mathbf{x}, t_\infty) = u^*$. However we also know, from Eqn. 10, that the worst case strain is computed using

$$\varepsilon(\mathbf{x}_{\text{worst}}, t_\infty) = \frac{D_\infty}{D_0}\varepsilon_0 = \frac{D_\infty}{D_0}\frac{\sigma_{\max}}{E_0}, \tag{39}$$

where ε_0 is the elastic strain due to the peak applied stress, $\sigma_{\max}$. Therefore from the definition of $\mathbf{x}_{\text{worst}}$, we can write

$$\varepsilon^* = \frac{D_\infty}{D_0}\frac{\sigma_{\max}}{E_0}, \tag{40}$$

We must now express the above equation in terms of the extremal relaxation coefficients, E_0 and E_∞. This is achieved by using Laplace analysis. Applying a Laplace transformation to Eqn. 2 leads to

$$\hat{D}(\xi) = \frac{1}{\xi^2 \hat{E}(\xi)}, \tag{41}$$

where $\hat{E}$ and $\hat{D}$ are the Laplace transforms of the relaxation and creep compliance functions respectively, and ξ is the transform parameter. From the known properties of Laplace transforms, we can write

$$D(t_\infty) = \lim_{\xi \to 0^+} \xi \hat{D}(\xi) = \lim_{\xi \to 0^+} \frac{1}{\xi \hat{E}(\xi)}. \tag{42}$$

Furthermore, any relaxation function can be described using a Prony series expression of the form

$$E(t) = E_\infty + \sum_{j=1}^{N_p} E_j e^{-t/\tau_j}, \tag{43}$$

where N_p is the number of Prony terms in the series, and the coefficients $\{E_j\}$ and $\{\tau_j\}$, are constants selected to fit the Prony series function to experimental results. Transforming the Prony series expression for $E(t)$ into the Laplace domain, we obtain

$$\begin{aligned} D(t_\infty) &= \lim_{\xi \to 0^+} \frac{1}{\xi \left(\frac{E_\infty}{\xi} + \sum_{j=1}^{N_p} \frac{\tau_j E_j}{\tau_j \xi + 1} \right)} \\ &= \frac{1}{E_\infty} \end{aligned} \tag{44}$$

Using a similar process, one can show that $D_0 = 1/E_0$. Inserting these identities into Eqn. 40, we obtain

$$\varepsilon^* = \frac{\sigma_{\max}}{E_\infty}, \tag{45}$$

From the definition of the partial worst-case strain, $\tilde{\varepsilon}$, we know that

$$\sigma_{\max} = \int_0^{t^*} E(t^* - s)\frac{\partial \tilde{\varepsilon}(s)}{\partial s}\mathrm{d}s. \tag{46}$$

Therefore we have

$$\begin{aligned}
\varepsilon^* &= \int_0^{t^*} \frac{E(t^* - s)}{E_\infty}\frac{\partial \tilde{\varepsilon}(s)}{\partial s}\mathrm{d}s \\
&= \int_0^{t^*} \frac{\partial \tilde{\varepsilon}(s)}{\partial s} + \int_0^{t^*} \left(\frac{E(t^* - s)}{E_\infty} - 1\right)\frac{\partial \tilde{\varepsilon}(s)}{\partial s}\mathrm{d}s \\
&= \tilde{\varepsilon}(t^*) + \int_0^{t^*} \left(\frac{E(t^* - s)}{E_\infty} - 1\right)\frac{\partial \tilde{\varepsilon}(s)}{\partial s}\mathrm{d}s
\end{aligned} \tag{47}$$

Since $E(t) > E_\infty$ for all t, $E(t^* - s)/E_\infty - 1 > 0$. It is also clear that $\tilde{\varepsilon}(s)$ is a monotonically increasing function of s, since $\tilde{\varepsilon}$ is the strain due to a constant applied load of $\sigma_{\max}$. Therefore $\frac{\partial \tilde{\varepsilon}(s)}{\partial s} > 0$ for all s. We can now write

$$\begin{aligned}
&\varepsilon^* = \tilde{\varepsilon}(\mathbf{x}_{\text{worst}}, t^*) + \Pi, \quad \text{where} \quad \Pi > 0 \\
\Rightarrow &\tilde{\varepsilon}(\mathbf{x}_{\text{worst}}, t^*) < \varepsilon^*,
\end{aligned} \tag{48}$$

Combining Eqn. 48 and 38, we get $\varepsilon(\mathbf{x}_{\text{worst}}, t^*) < \varepsilon^*$, and therefore the proof is complete.

This proves conclusively that the worst-case approach employed in the examples provides a reliable upper bound on all possible deflections. It also shows that although this approach is computationally inexpensive (since the worst-case analysis requires the solution of just one linear system, similar to the elastic case), the actual viscoelastic deflection will be less than the target deflection value, which, as we showed earlier, results in a suboptimal design. Similarly, it has been shown that assuming linear elasticity leads to an infeasible structure that is insufficiently stiff, and therefore exceeds the target deflection. The performance of the optimal viscoelastic design will be bound on either side by these two extreme cases.

5.2. Extension to Multi-Dimensional Problems Using Finite Element Analysis

The proofs presented in the previous section apply narrowly to the one-dimensional case involving a linear viscoelastic structure subject to unidirectional axial loading. However, in practice, most computational structural optimization methods involve two- or three dimensional structures with complex geometries, and which are modeled using finite element analysis, or some other form of discretization. In the current section, we show how the underlying derivations for each of the proofs presented earlier, can be adapted to apply to two-and three-dimensional problems of arbitrary geometry. Specifically we derive a proof of the proposition $u(\mathbf{x}_{\text{elastic}}, t^*) > u^*$ for a generalized structure of arbitrary geometry and dimension using a generic finite element formulation (note that since all equations in this section pertain to the elastic design $\mathbf{x}_{\text{elastic}}$, we hereafter omit the $\mathbf{x}$ variable, as was done in the previous section). Derivation of the finite element analogs of the remaining proofs pertaining to the worst case design, are left as an exercise for the reader.

For the general problem, we restrict the applied loads to the class of proportional loads, meaning only the load magnitude varies with time, while the load pattern or *profile* remains constant. Mathematically this implies that all applied loads $f(\mathbf{X}, t)$ must satisfy

$$f(\mathbf{X}, t) = \alpha(t) f(\mathbf{X}), X \in \mathbb{R}^d, d \in \{2, 3\} \tag{49}$$

where the variable $\mathbf{X}$ represents the spatial coordinate in two- or three-dimensional space, and $\alpha(t)$ is a scalar function indicating the relative magnitude of the applied force at time t. In finite element terms all applied forces can be represented by

$$\mathbf{F}(t) = \alpha(t)\mathbf{F}_0 \tag{50}$$

where $\mathbf{F}$ is the consistent force vector, and $\mathbf{F}_0$ is a constant vector describing the load pattern. As in the previous section, we again restrict the applied forces so that $\alpha(t) \geq 0$ for all t. Finally, we require that all loads be concentrated loads that can be represented as single point loads in the finite element model (it is assumed that the deflection constraint is evaluated at the location of the applied load). This restriction is necessary since the general proposition we seek to prove does not hold in general for all distributed

and multi-point loads. Under the generic finite element formulation, all applied stresses, $\sigma(t)$, from Section 5.1 are replaced with applied forces $\mathbf{F}(t)$ and all viscoelastic strains, $\varepsilon(t)$ are replaced with viscoelastic displacements $u(t)$. Using a derivation similar to that which was used to prove lemma 2 (Eqn. 13) above, it can be shown that

$$\text{if } \alpha(t) \geq 0 \text{ for all } t, \text{ then } u(t) > 0 \text{ for all } t > 0 \tag{51}$$

We begin by expressing the structure's equilibrium equation in generic finite element terms using a semi-discrete FEM form in which the spatial domain is discretized, but the time domain remains continuous. We first note that

$$\begin{aligned} \mathbf{f}_e(t) &= \int_{\Omega_e} \mathbf{B}^{\mathrm{T}} \boldsymbol{\sigma}(t) \mathrm{d}V \\ &= \int_0^t \int_{\Omega_e} \mathbf{B}^{\mathrm{T}} \mathbf{C}(t-s) \frac{\partial \boldsymbol{\varepsilon}(s)}{\partial s} \mathrm{d}V \mathrm{d}s \end{aligned} \tag{52}$$

where $\mathbf{f}_e$ is the vector of applied nodal forces corresponding to element e, Ω_e is the volume occupied by element e, and $\mathbf{B}$ is the strain displacement matrix for element e. In the second line above, we have substituted the general Boltzmann formula for the internal stress tensor, $\boldsymbol{\sigma}$, (Eqn. 4). The strain displacement matrix is defined such that, $\boldsymbol{\varepsilon} = \mathbf{B}\mathbf{u}_e$, where $\mathbf{u}_e$ is the vector of nodal displacements for element e. Therefore we can write

$$\begin{aligned} \mathbf{f}_e(t) &= \int_0^t \int_{\Omega_e} \mathbf{B}^{\mathrm{T}} \mathbf{C}(t-s) \mathbf{B} \frac{\partial \mathbf{u}_e(s)}{\partial s} \mathrm{d}V \mathrm{d}s \\ &= \int_0^t \mathbf{k}_e(t-s) \frac{\partial \mathbf{u}_e(s)}{\partial s} \mathrm{d}s, \end{aligned} \tag{53}$$

where $\mathbf{k}_e$ is the element stiffness matrix, which depend on t due to viscoelasticity, and can be computed using

$$\mathbf{k}_e = \int_{\Omega_e} \mathbf{B}^{\mathrm{T}} \mathbf{C}(t-s) \mathbf{B} \mathrm{d}V. \tag{54}$$

When we combine the equilibrium equations from all elements through the process of assembly, we arrive at the following global equilibrium equation.

$$\mathbf{F}(t) = \int_0^t \mathbf{K}(t-s)\frac{\partial \mathbf{u}(s)}{\partial s}\mathrm{d}s, \tag{55}$$

where $\mathbf{u}$ is the global vector of nodal displacements. The viscoelastic displacement used to evaluate the constraint, is given by

$$u = \mathbf{L}^{\mathrm{T}}\mathbf{u}, \tag{56}$$

where $\mathbf{L}^{\mathrm{T}}$ is the unit basis vector whose entries are zero except in the location corresponding to the node where the displacement is constrained (i.e. $\mathbf{L}^{\mathrm{T}} = [0 \ ... \ 0 \ 1 \ 0 \ ...0]^{\mathrm{T}}$). Using this finite element formulation, we seek to prove that $u(\mathbf{x}_{\mathrm{elastic}}, t^*) > u^*$, where u^* is the target displacement specified in the design optimization problem.

The elastic deflection, $u_0(\mathbf{x}_{\mathrm{elastic}}, t^*)$, is obtained by solving the following linear elasticity equation

$$\mathbf{F}(t^*) = \mathbf{K}_0(\mathbf{x}_{\mathrm{elastic}})u_0(\mathbf{x}_{\mathrm{elastic}}, t^*), \tag{57}$$

where $\mathbf{K}_0(\mathbf{x}_{\mathrm{elastic}})$ is the global stiffness matrix corresponding to the design described by $\mathbf{x}_{\mathrm{elastic}}$ at time $t = 0$. Note that since all variables used in the remainder of the proof correspond to the design $\mathbf{x} = \mathbf{x}_{\mathrm{elastic}}$, we hereafter omit the $\mathbf{x}$ value in all subsequent equations for increased clarity. Combining equations 55 and 57, we can equate the two expressions for $\mathbf{F}(t^*)$ as follows.

$$\mathbf{K}_0\mathbf{u}_0(t^*) = \int_0^{t^*} \mathbf{K}(t-s)\frac{\partial \mathbf{u}(s)}{\partial s}\mathrm{d}s, \tag{58}$$

Multiplying both sides of the equation by $\mathbf{L}\mathbf{K}_0^{-1}$, we obtain

$$u_0(t^*) = \int_0^{t^*} \frac{E(t-s)}{E_0}\frac{\partial u(s)}{\partial s}\mathrm{d}s, \tag{59}$$

Now recall that the elastic design, $\mathbf{x}_{\text{elastic}}$, corresponds to the structure that is designed so that, when evaluated based on the assumption of elasticity, its deflection satisfies the constraint $u_0(\mathbf{x}_{\text{elastic}}, t^*) = u^*$. Therefore we can replace the quantity $u_0(t^*)$ above with the target deflection value, u^*. For notational brevity, we also re-introduce the variable $\theta(s) = E(t^* - s)$. Consequently Eqn. 59 becomes

$$\begin{aligned} u^* &= \int_0^{t^*} \frac{\theta(s)}{E_0} \frac{\partial u(s)}{\partial s} \mathrm{d}s \\ &= \int_0^{t^*} \frac{\partial u(s)}{\partial s} \mathrm{d}s - \int_0^{t^*} \left(1 - \frac{\theta(s)}{E_0}\right) \frac{\partial u(s)}{\partial s} \mathrm{d}s \\ &= u(t^*) - \int_0^{t^*} \left(1 - \frac{\theta(s)}{E_0}\right) \frac{\partial u(s)}{\partial s} \mathrm{d}s \end{aligned} \tag{60}$$

As in the analogous proof from the previous section, we now rearrange to isolate the variable $u(t^*)$, and integrate by parts to obtain

$$\begin{aligned} u(t^*) &= u^* + \left[\left(1 - \frac{\theta(s)}{E_0}\right) u(s)\right]_0^{t^*} - \int_0^{t^*} \left(-\frac{\partial \theta(s)}{\partial s}\right) u(s) \mathrm{d}s \\ &= u^* + \left(1 - \frac{\theta(t^*)}{E_0}\right) u(t^*) + \int_0^{t^*} \frac{\partial \theta(s)}{\partial s} u(s) \mathrm{d}s \end{aligned} \tag{61}$$

Note that, as before, the term $\left(1 - \frac{\theta(0)}{E_0}\right) u(0)$ vanishes since $u(0) = 0$. The terms that remain are all positive, and therefore we can conclude that

$$u(t^*) = u^* + \Pi, \quad \text{where } \Pi > 0. \tag{62}$$

Therefore $u(\mathbf{x}_{\text{elastic}}, t^*) > u^*$ and the proof is complete. This proof applies to any structure modeled using finite element discretization and subject to unidirectional, proportional, concentrated loading. Similar analogs can be derived for each of the proofs presented in Section 5.1.

6. Numerical Examples

To demonstrate that Proposition (9) holds in practice, we optimize the seven-bar truss structure shown in Figure 2. The structure is comprised of

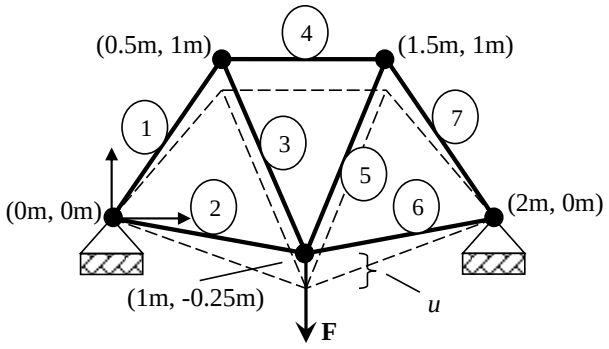

Figure 2: Geometry and boundary conditions of the viscoelastic truss structure to be optimized

viscoelastic material whose creep and relaxation functions are given by Prony series of the form

$$E(t) = E_\infty + \sum_{i=1}^{N_p} E_i e^{-t/\tau_i}; \quad D(t) = D_\infty - \sum_{i=1}^{Np} D_i e^{-t/\tau_i}, \tag{63}$$

where N_p is the number of Prony terms in the series. For these examples, we use a two-term Prony series for each function, with the Prony coefficients given in Table 1.

Relaxation $[\times 10^9 \text{Pa}]$		**Creep compliance** $[\times 10^{-10} \text{Pa}^{-1}]$		**Retardation times**[s]	
E_∞	2.0	D_∞	5.0	–	–
E_1	1.0	D_1	1.0	τ_1	100
E_2	2.0	D_2	2.0	τ_2	1000

Table 1: Prony series coefficients used in the relaxation and creep compliance functions

The structure is optimized by varying the cross-sectional areas, A_i, of the truss members in order to achieve minimum mass, subject to a constraint on the displacement at the point of the applied load. In all optimization procedures, the structure is modeled using 7 truss elements, and the optimization problem is solved numerically using the method of moving asymptotes [13].

In the first example, the applied load is constant so that $||\mathbf{F}(t)|| = 10^6 N$, for $0 \leq t \leq 1000s$. The maximum allowable displacement is set at $u_{\max} = 0.25m$. Due to assumed manufacturing constraints, a lower bound is set on the individual bar cross-sections such that $A_{\min} = 5 \times 10^{-4} m^3$. The optimization problem can be written as follows.

$$\begin{aligned} \min_{\{A_i\}} \quad & \sum_{i=1}^{N_{\text{bar}}} A_i l_i \\ \text{subject to:} \quad & u(t^*) \leq u_{\max} \\ & \int_0^t \mathbf{K}(t-s) \frac{\partial \mathbf{u}(s)}{\partial s} \mathrm{d}s - \mathbf{F}(t) = \mathbf{0} \\ & A_i \geq A_{\min} \ \text{ for all } \ i \end{aligned} \tag{64}$$

Here, l_i is the length of truss element i, N_{bar} is the number of truss elements in the structure, and t^* is the target time at which the constraint function is evaluated, so that $N_{\text{bar}} = 7$ and $t^* = 1000s$. The above optimization problem is solved using the three approaches described in Section 3. In the first optimization, the structure is assumed to be elastic, in the second optimization, we assume worst-case viscoelastic displacement, and in the third optimization we employ time-dependent viscoelastic analysis based on Eqn. 10.

Table 2 describes the optimized designs obtained from each of the three approaches. (Note that the bar numbers in the table correspond to the circled numbers in Fig. 2. The sizes of bars 5-7 can be deduced from symmetry.) As predicted by the earlier proofs, the worst-case design is the heaviest, while the elasticity-based design is the lightest, with the viscoelastic design lying between these two extremes. Figure 3 shows the viscoelastic displacement histories of each of the optimized designs when evaluated using time-dependent viscoelastic analysis. As seen in the plot, only the viscoelastic design has a final deflection that is equal to the target deflection of $u = 0.25m$. By contrast the deflection of the elastic design exceeds the target deflection by a significant margin, thus rendering the elastic design infeasible. Similarly, the deflection of the worst-case design is significantly lower than the target deflection, indicating that this design is suboptimal.

In the second example, we optimize the same structure subject to the sinusoidal time-varying load shown in Fig. 4. In this problem, the maximum

	Cross-sectional area $[\times 10^{-3} m^2]$				**Total mass [kg]**
	Bar 1	Bar 2	Bar 3	Bar 4	
Elasticity	1.283	0.500	1.229	1.015	7.10
Worst case	3.419	0.500	3.277	2.705	17.44
Viscoelastic	2.895	0.500	2.775	2.291	14.91

Table 2: Design specifications for the optimized truss structures designed for the constant load case (Note that mass density is assumed to be $\rho = 850 kg/m^3$)

allowable deflection is set to $u_{\max} = 0.2m$, and the target time is $t^* = 4000s$. For the viscoelastic analysis, the time domain is discretized using a forward Euler time-marching scheme, with 250 time steps.

Table 3 describes the optimized design obtained using each of the three optimization approaches. As in the constant load example, the elastic design is the lightest, while the worst-case design is significantly heavier. Figure 5 shows the displacement histories of each of the three designs. Here again, we see that only the viscoelastic design has a deflection that is equal to the target value, whereas the elastic design is infeasible, and the worst-case design is suboptimal. As expected, these mass and displacement characteristics are fully consistent with the predictions made by the proofs derived for both constant and time-varying loads.

	Cross-sectional area $[\times 10^{-3} m^2]$				**Total mass [kg]**
	Bar 1	Bar 2	Bar 3	Bar 4	
Elasticity	1.639	0.500	1.571	1.297	8.82
Worst case	4.309	0.500	4.130	3.410	21.75
Viscoelastic	2.913	0.500	2.791	2.305	14.99

Table 3: Design specifications for the optimized truss structures designed for the time-varying load case

7. Conclusions

The proofs presented above demonstrate the importance of accurately accounting for viscoelastic behavior in design optimization algorithms. As

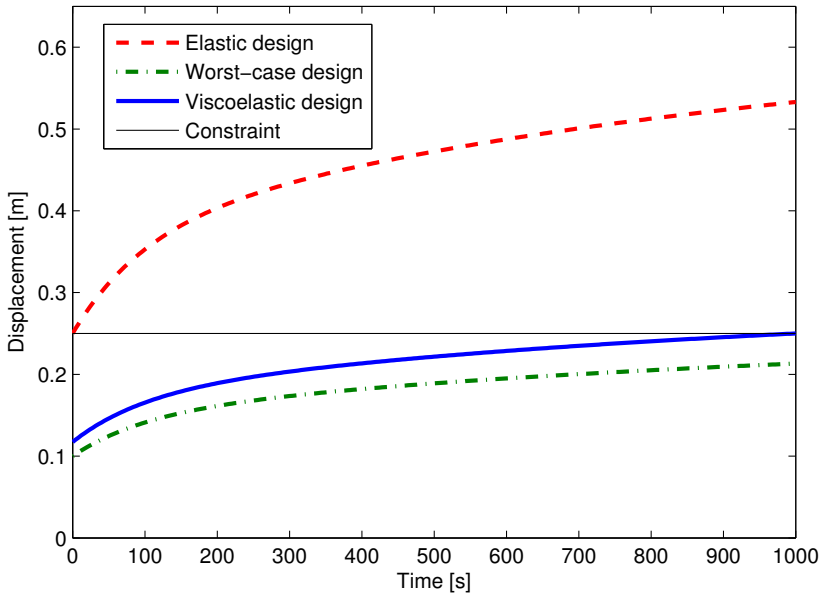

Figure 3: Viscoelastic displacement histories of the structures optimized for the constant load

shown in Section 5.1 standard optimization techniques based on linear elastic analysis can lead to structures that are infeasible when viscoelasticity is taken into account. Alternatively, designers may forgo the detailed time-dependent analysis required to accurately model the viscoelastic response of the structure and instead simply model the worst-case scenario of maximum viscoelastic deformation. While this option has low computational cost, it can lead to suboptimal designs that fail to exploit potential weight savings. Depending on the operating environment (particularly the temperature) and the time-scale of the loading cycle, viscoelastic analysis may be necessary for a wide range of engineering materials from concrete, asphalt and metals to synthetic polymers. For this reason, more work needs to be done to better harness the power of viscoelastic analysis for the purpose design optimization, and understand the impact of viscoelasticity on the long-term performance of optimized designs.

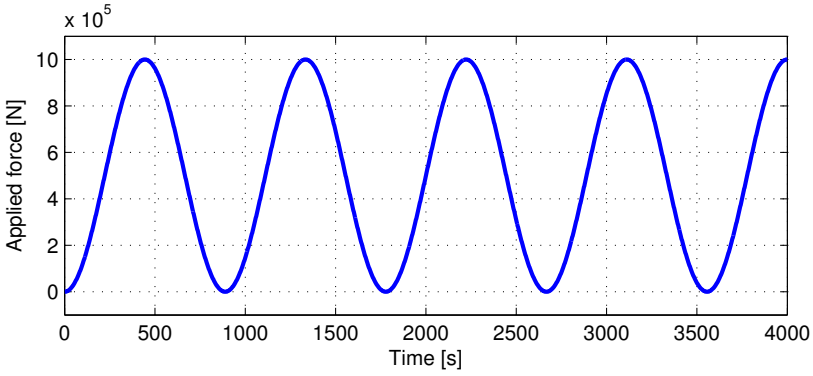

Figure 4: Applied force history for the time-varying viscoelastic optimization problem

Acknowledgments

The authors wish to acknowledge the financial support of the National Science Foundation under grant number CMMI-1334857.

Appendix A. A Note on Suboptimality

It can also be shown that the scenario in which $|u(\mathbf{x}, t^*)| < |u^*|$, where the deflection constraint is inactive due to the over-design of the structure, is suboptimal. In other words, it is possible to find a lighter design that also satisfies the deflection constraint. To prove this, we select an arbitrary design represented by $\bar{\mathbf{x}}$ such that

$$\bar{x}_i \leq x_{\text{worst}\,i} \tag{A.1}$$

for all elements, i, in the structural model. Let u be the magnitude of the deflection at the location of the deflection constraint. The deflection u is a continuous function of $\mathbf{x}$, therefore from the gradient theorem

$$u(\bar{\mathbf{x}}) = u(\mathbf{x}_{\text{worst}}) + \int_{\gamma[\bar{\mathbf{x}},\mathbf{x}_{\text{worst}}} \frac{\partial u}{\partial \mathbf{x}}^{\mathrm{T}} \,\mathrm{d}\mathbf{r}, \tag{A.2}$$

where $\mathbf{r} = \bar{\mathbf{x}} - \mathbf{x}_{\text{worst}}$, and γ is the linear path between the points $\bar{\mathbf{x}}$ and $\mathbf{x}_{\text{worst}}$ in the design space (Note that the proof also holds for any arbitrary path, γ,

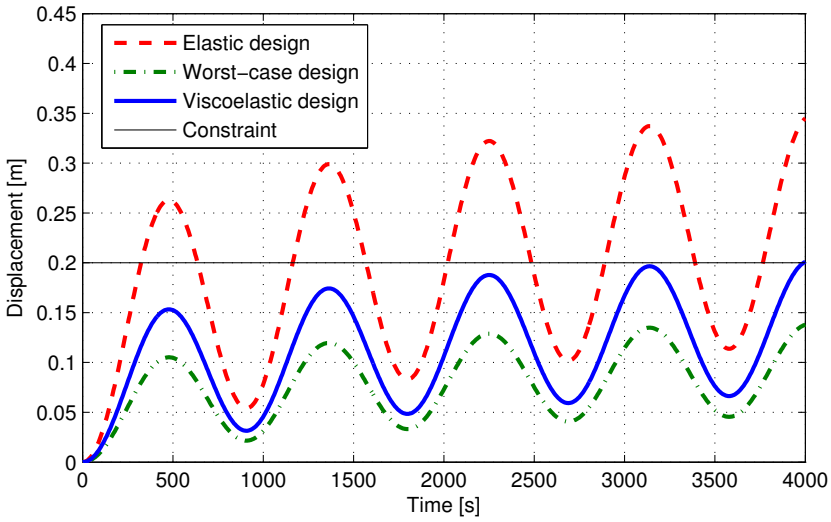

Figure 5: Viscoelastic displacement histories of the structures optimized for the sinusoidal time-varying load

between $\bar{\mathbf{x}}$ and $\mathbf{x}_{\text{worst}}$ in which all x values increase monotonically along the path.) Only two possibilities exist for $u(\bar{\mathbf{x}})$:

$$\begin{aligned} &\boldsymbol{(a)} \quad u(\bar{\mathbf{x}}) \leq u^* \\ &\boldsymbol{(b)} \quad u(\bar{\mathbf{x}}) > u^* \end{aligned} \tag{A.3}$$

If $\boldsymbol{(a)}$ is true, this means that the design given by $\bar{\mathbf{x}}$ satisfies the constraint, and also has a lower mass than the worst-case design due to Eqn. A.1, therefore the worst case design is suboptimal. Conversely, if $\boldsymbol{(b)}$ is true, then the design represented by $\bar{\mathbf{x}}$ breaches the constraint and we have

$$u(\bar{\mathbf{x}}) > u^* \geq u(\mathbf{x}_{\text{worst}}). \tag{A.4}$$

Therefore, from the intermediate value theorem, there must be some design, $\mathbf{x}^* \in \gamma[\bar{\mathbf{x}}, \mathbf{x}_{\text{worst}}$ such that $u(\mathbf{x}^*) = u^*$. Equivalently, there exists some $\beta \in (0, 1)$ such that

$$u(\mathbf{x}^*) = u^* \text{ where } \mathbf{x}^* = \mathbf{x}_{\text{worst}} + \beta \mathbf{r} \tag{A.5}$$

In this case, the design $\mathbf{x}^*$ has a lower mass than the worst-case design, while still satisfying the deflection constraint. Therefore the worst-case design must be suboptimal.

[1] J. Prasad, A. Diaz, Viscoelastic material design with negative stiffness components using topology optimization, Struct. Multidisc. Optim. 38 (2009) 583–597.

[2] E. Andreassen, J. Jensen, Topology optimization of periodic microstructures for enhanced dynamic properties of viscoelastic composite materials, Struct. Multidisc. Optim. 49 (2013) 695–705.

[3] A. El-Sabbagh, A. Baz, Topology opitmization of unconstrained damping treatments for plates, Engrg. Optim. 46 (2014) 1153–1168.

[4] Z. Liu, H. Guan, W. Zhen, Topology optimization of viscoelastic materials distribution of damped sandwich plate composite, Appl. Mech. Mater. 347–350 (2013) 1182–1186.

[5] W. Chen, S. Liu, Topology optimization of microstructures of viscoelastic damping materials for a prescribed shear modulus, Struct. Multidisc. Optim. 50 (2014) 287–296. doi:10.1007/s00158-014-1049-3.

[6] K. Jensen, P. Szabo, F. Okkels, Topology optimization of viscoelastic rectifiers, Appl. Phys. Lett. 100 (2012) 1–4.

[7] K. James, H. Waisman, Topology optimization of viscoelastic structures using a time-dependent adjoint method, Comput. Methods Appl. Mech. Engrg. 285 (2015) 166–187.

[8] M. Deng, J. Zhou, Effects of temperature and strain level on stress relaxation behaviors of polypropylene sutures, J. Mater. Sci.: Mater Med 17 (2006) 365–369.

[9] S. Marques, G. Creus, Computational Viscoelasticity, Springer, 2012.

[10] H. Brinson, L. Brinson, Polymer Engineering Science and Viscoelasticity, Springer, 2008.

[11] M. Sedef, E. Samur, C. Basdogan, Real-time finite-element simulation of linear viscoelastic tissue behavior based on experimental data, IEEE Computer Graphics and Applications 26 (2006) 28–38.

[12] D. Gutierrez-Lemini, Engineering Viscoelasticity, Springer, 2014.

[13] K. Svanberg, The method of moving asymptotes - a new method for structural optimization, Int. J. Numer. Meth. Optim. 24 (1987) 359–373.